Environ Earth Sci (2016) 75:823
DOI 10.1007/s12665-016-5522-8

ORIGINAL ARTICLE

Stream sediment geochemistry of the upper Cheyenne River watershed within the abandoned uranium mining region of the southern Black Hills, South Dakota, USA

Rohit K. Sharma[1] · Keith D. Putirka[2] · James J. Stone[1]

Received: 23 June 2015 / Accepted: 29 February 2016 / Published online: 29 April 2016

Abstract Abandoned uranium (U) mine workings and tailings deposits are found throughout the southern Black Hills of South Dakota. The close proximity of the mine sites to the Cheyenne River (CR) appears to promote elevated metal and radionuclide transport within the watershed, however, the extent of their contribution is unknown. Sixty sediment and soil samples were collected from potentially impacted locations within the watershed to elucidate contaminant occurrence and transport mechanisms. The degree of sediment contaminant impacts were assessed by establishing enrichment factors (EF) and pollution load indices (PLI) criterion as compared to non-mining impacted reference sites. Herron classifications suggest that the sediments collected from the southern Black Hills are immature, consistent with the presence of detrital feldspar. Generally, sediment Sr content were found depleted and intermittently enriched in Rb/Sr ratios compared to upper continental crust concentrations, suggesting physical weathering mechanisms predominate within the CR catchment up gradient of the Angostura Reservoir. Increasing EF and PLI indices coupled with low strontium (Sr) values suggest sediment contamination found along the CR and Angostura Reservoir delta appear attributed to anthropogenic activities and not natural weathering processes.

✉ James J. Stone
james.stone@sdsmt.edu

[1] Department of Civil and Environmental Engineering, South Dakota School of Mines and Technology, Rapid City, SD 57701, USA

[2] Department of Earth and Environmental Sciences, California State University Fresno, Fresno, CA 93740, USA

Keywords Geochemistry · Stream sediments · Uranium · Mineralogy · Chemical weathering · Enrichment factor · Pollution load index

Introduction

History of uranium (U) mining in the southern Black Hills of South Dakota US dates to the 1950s. Uranium deposits were found and mined from four primary areas: Edgemont area, Carlile area, Hulett Creek area, and Elkhorn Creek area (Fig. 1). Uranium deposits were discovered in the Black Hills in Craven Canyon north of Edgemont, South Dakota (Robinson and Gott 1958), with U production in the Edgemont area the highest among all the areas combined. There are an estimated 142 abandoned U mine and prospect sites in the Edgemont area of South Dakota (SD) (Braddock 1955). These U deposits are present in the rocks of Inyan Kara Formation as a carnotite, tyuyamunite, metatyuyamunite, corvusite, and associated secondary U and vanadium (V) minerals. These minerals are deposited as a mineralizing solution through the permeable Inyan Kara Group (Robinson and Gott 1958). Uranium and V are accumulated as front roll deposits in the Cretaceous rocks and formed in reducing environment close to the surface (DeWitt and Buscher 1988). Most of the openings at the mine site are shaft, open pit, and trench (DeWitt and Buscher 1988). To date, very little reclamation has been done in these mined areas. Abandoned U mines are scattered throughout the Edgemont U district with mine tailings still found adjacent to mined areas. These tailings are a continued source of radiological elements, while the close proximity of these tailings to the Cheyenne River may promote the contaminant migration into the southern Black Hills watersheds.

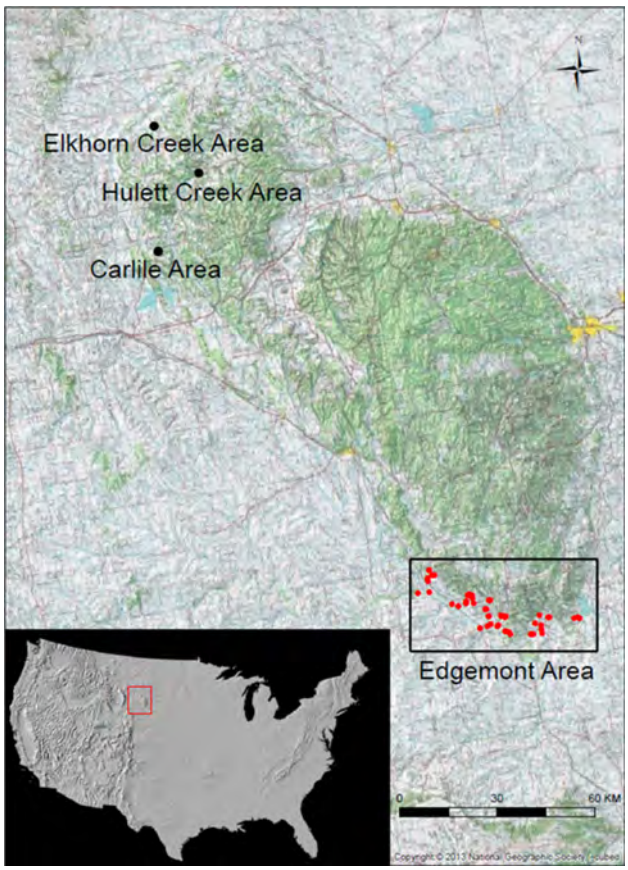

Fig. 1 Location map showing study area (*boxed*) and principle uranium mining areas within the Black Hills of SD: Edgemont, Carlile, Hulett Creek, and Elkhorn Creek

Several studies have evaluated the environmental hazard of abandoned mines in the U mining district north of Edgemont (Davis and Webb 1999; Hall 1982; Webb et al. 1995, 1998). Rahn and Hall (1982) and Hall (1982) documented 24 abandoned U mines within the Edgemont district. Rahn et al. (1996) focused on water quality impacts relating to abandoned mining in the region, and reported dissolved uranium exceeding 2.6 mg/L at several sites. In a similar study employing a watershed approach, Davis and Webb (1999) evaluated water-quality impacts from abandoned mines within the Bear Butte Creek basin of the northern Black Hills, and the headwaters of the Driftwood Creek basin within the uranium mining district of the southern Black Hills. Their study reported water-quality impacts were limited to the Strawberry Creek and the Bear Butte Creek, while for Driftwood Creek, surface water-quality impacts were limited to a stock pond down-gradient from abandoned U mines. Webb et al. (1995) reported 2 mg/L U found within mine pit waters of the southern Black Hills region.

Transport of metals within a river system may occur due to physical or chemical transport processes. In the Black Hills region, solid phase sediments are primarily composed of silicate and secondary clay minerals, such as aluminosilicate clay minerals. Metals in solid phase are present in the river sediments in very low concentrations and typically bound within these aluminosilicate clay minerals, and as a result, may show little fractionation during weathering processes (Windom 1988). Furthermore, when metals in solution come in contact with the stagnant water bodies such as lakes and reservoirs, they are quickly removed from the water column via sedimentation, and often concentrated within lake and reservoir bottom sediments. Pollution from the abandoned mines is of paramount environmental concern in the Black Hills region, as the heavy metals may be transported from the mining areas to the water resources down gradient, leading to environmental degradation.

The objectives of this study were (1) to determine the presence of heavy metals and radionuclides that may have been transported from abandoned U mining areas of the southern Black Hills, specifically within the Cheyenne River watershed above the Angostura Reservoir; (2) to elucidate transport mechanisms of the contaminants; and (3) to assess the degree of potential contamination within the watershed soils and sediments.

Study area

The study area is situated in the southern Black Hills of South Dakota. The U mining area is commonly referred to as the 'Edgemont U district' located 25 km north of Edgemont in Fall River County (Fig. 1). The sampling area lies south of Dewey-Minnekahta road, north of Edgemont, and west of Angostura Reservoir. The land use of study area is mostly grazing, wilderness, and outdoor recreation. The town of Edgenont is approximately 30 km west of the Angostura Reservior. The Black Hills Wild Horse Sanctuary is approximately 12 km west of the Angustora Reservior.

The Cordilleran foreland basin in the North America is considered as one of the major basement deformation along the orogenic belt in the world. It is located between south of the Colorado Plateau and the Rocky mountain in south Canada. The western part of the basin is bounded by large scale uplifts of deep basement. High angle normal fault and reverse fault are predominant structures within the Black Hills tectonic unit of Cordilleran foreland basin, which resulted from the vertical movement of Precambrian basement blocks (Osterwald and Dean 1961). The Black Hills uplift in western South Dakota consists of central Precambrian basement surrounded by sedimentary rocks of Paleozoic and Mesozoic ages. The Precambrian core in Black Hills is granitic in center and metamorphic around its

margin (Sales 1968). Uranium deposits in Black Hills are close to the igneous structures (Osterwald and Dean 1961). Numerous studies have identified sources of U in the black shale in Black Hills region. Finnell and Parrish (1958) suggested that U deposits may have been influenced by igneous intrusions and characteristic of host rocks. The host rock of these U deposits are Lakota and Fall River Formations of the lower Cretaceous age Inyan kara Group. These formations consist of intermediate carbon rich sedimentary rocks with thinly bedded mudstone and shale. The U deposits in the Inyan kara Group are considered roll-front deposits, formed by the introduction of U rich oxidizing groundwater into reduced sediment beds along basin margins (IAEA 1985).

Geology of the study area consists of sandstone of the Lakota and Fall River Formations of early Cretaceous age Inyan Kara Group, which forms a major hogback surrounding Black Hills. I Dead Canyon, Dewey Mines, and Chilson Canyon nyan Kara Group also consists of intermediate carbon rich sedimentary rocks. In the southern Black Hills, according to Robinson and Gott (1958), the Inyan Kara Group dips gently away from the core of the uplift where faults are rare. The Lakota Formation is overlain by the Fall River Formation, and unconformably overlies the Morrison Formation. The Lakota Formation consists of lenticular beds of sandstones including conglomerate, sandy claystone, and carbonaceous shale and ranges in thickness between 30.5 and 152 m. The Fall River Formation consists of well bedded, fine-grained sandstone, with some siltstone and claystone with a maximum thickness of about 61 m (Rich 1981). The Fall River Formation and Lakota Formation are separated from each other by a sharp lithological break (Robinson and Gott 1958).

Methods

Sample collection

Three groups of samples were considered for this study: mine tailings, river drainages, and Angostura Reservoir. Mine tailings samples were collected from several abandoned U mines located within the southern Black Hills region. River sediment samples were collected from the major drainages containing abandoned U mines and prospects. Angostura Reservoir samples were shallow depth samples collected from the Cheyenne River delta. The delta samples were collected from a depth of about 1 m below the water column where sediment accumulation is considered greater. A total of 60 soil and sediment samples were collected from various locations from the Cheyenne River (CR) (19 samples) and its drainages, namely Red Canyon (RC) (nine samples), Sheep Canyon (SC) (two samples), Chilson Canyon (CC) (four samples), Dead Canyon (DC) (12 samples), various abandoned U mines (Mines) (seven samples), five soil samples, and Angostura Reservoir delta (ANG) (three samples), in the southern Black Hills (Fig. 2). Three bottom lake delta sediments were collected from Angostura Reservoir using a 122 cm length suction coring device (Wildco 2400-B20KB), with cores collected within internal 4.31 cm diameter plexiglass tube. Sediment cores were collected near channel inflow where the sedimentation rate was considered higher. Core samples were sliced into 2–3 cm segments.

Fifty-seven soil and sediment samples were collected within the Cheyenne River catchment above Angostura Reservoir to understand contaminant transport mechanism of the watershed. Samples were collected from within the channel where sediment accumulation was considered high. Soil and sediment samples were collected using a hand auger. All samples were placed in a 120 mL whirl–pak bags and stored at 4 °C prior to analysis.

Laboratory analysis

All samples were screened in the laboratory and any cobble were removed manually. Organic matter content was determined by loss on ignition (LOI) method following Heiri et al. (2001). Pellets of 1 mm in diameter were prepared with 0.9 gm of sample (soil, sediment, and core slices) that were individually ground using mortar and pestle, and mixed with 0.1 gm of ultra-bind. Pressed powder pellets were analyzed for major and trace elements (Ag, As, Ca, Cr, Cu, Fe, Mn, Mo, Ni, Pb, Rb, SiO_2, Sr, Ti, U, V, and Z) using a Bruker Tracer III-SD hand-held X-ray fluorescence spectrometry (XRF) instrument.

Statistical methods

Inter-element correlations were determined using Pearson moment correlations (SigmaPlot, Systat Software, San Jose, CA). The significance of statistical test was set at $p < 0.04$.

Evaluation methods

Heavy element accumulation in river sediments can be influenced by factors such as geology, sediment transport, and anthropogenic activity. The degree of contamination found within sediment samples collected was determined using enrichment factor (EF) (Zoller et al. 1974; Sinex and Helz 1981) and pollution load index (PLI) (Tomlinson et al. 1980). EF is expressed by the following equation

$$\mathrm{EF} = \frac{\left(\frac{X}{\mathrm{Al}}\right)\ \mathrm{Sample}}{\left(\frac{X}{\mathrm{Al}}\right)\ \mathrm{Pierre\ Shale}}, \quad (1)$$

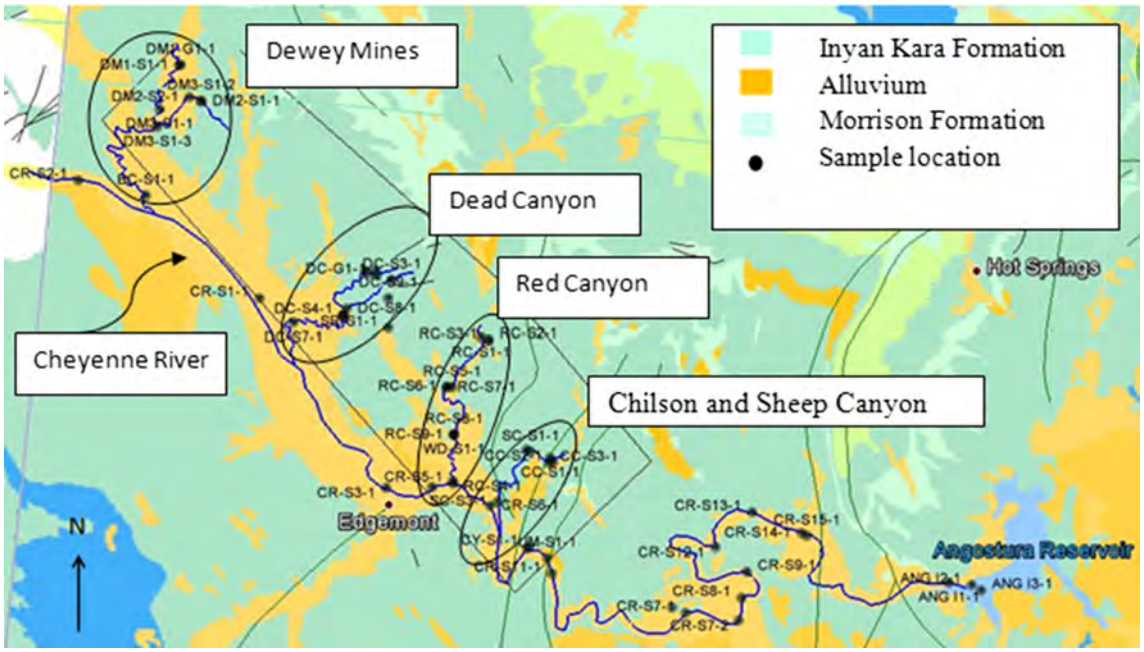

Fig. 2 Sampling location Dewey Mines (DM), Cheyenne River (CR), Red Canyon (RC), Chilson Canyon (CC), Sheep Canyon (SC), and Angostura Reservior (ANG) and primary geologic formations of southern Black Hills region. *Black dots* represent sampling locations for study

where X is the elemental concentration compared to Al used as a reference element because of it's an immobile element and a major constituent of clay mineral. Pierre Shale value was from Schultz et al. (1980). The EF classification consists of five groups describe as follows (Mmolawa et al. 2011):

<2 = depleted;
2–5 = moderately enrichment;
5–20 = significant enrichment;
20–40 = very high enrichment;
>40 = extremely enrichment.

PLI proposed by Tomlinson et al. (1980) was used as an indicator of pollution caused by anthropogenic activities. PLI is determined by:

$$\mathrm{PLI} = (\mathrm{CF1} \times \mathrm{CF2} \times \mathrm{CF3} \times \cdots \times \mathrm{CFn})1/n, \quad (2)$$

where CF is contamination factor and n is number of heavy metals. Contamination factor is defined as metal concentration in sediments divided by the background values of metal within Pierre Shale (Schultz et al. 1980). The PLI value less than 1 indicates minor pollution while PLI greater than 1 indicates pollution.

Results and discussion

Major elements

Major oxide determination is helpful to classify the rock types and construct of a chemical variation diagram. Bulk elemental geochemistry of major elements was plotted against Al_2O_3 which shows the most chemical variation among all oxides ranges from 9.3 to 35.9 % in the variation diagram (Fig. 3). Pierre Shale (Schultz et al. 1980) and Harney Peak Biotitic Granite (HPBG) (Duke et al. 1992) values were included within the variation diagram as representative comparisons. Bottom sediments collected from Angostura delta were low in SiO_2 and varied from 44.5 % (27–30 mm) to 62 % (30–33 mm), with higher concentrations at deeper depths. This is indicative of sediment fractionation within the water column, with enrichment of phyllosilicates at shallow depths and sand rich at depth (Das et al. 2006) (Fig. 3). Cheyenne River sediments were comparatively low in Al_2O_3 than other samples collected from Angostura watershed, while upstream sediments of Cheyenne River were low in CaO, P_2O_5, and K_2O, and higher in Fe_2O_3 and TiO_2. SiO_2 was depleted and K_2O, MgO, Fe_2O_3, and TiO_2 were enriched in most samples compared to Pierre Shale and HPBG. It has been suggested that the Al_2O_3 in sediments increases towards finer grain and SiO_2 towards coarse grains (Das and Haake 2003; Vital and Stattegger 2000) (Fig. 3). Elements like Fe_2O_3, TiO_2, and K_2O exhibit behavior similar to Al_2O_3, suggesting a tendency to be enriched in finer grains. The smoothing trends for (−ve), Fe2O3 (+ve), CaO (−ve), and TiO2 (+ve) with Al_2O_3 indicate the presence of clay minerals in sediments, while correlations between Fe_2O_3 and TiO_2 to Al_2O_3 appear due to biotite enrichment. In clay sediments CaO was negatively correlated with Al_2O_3 due to Ca removal during sediment transport. During chemical and

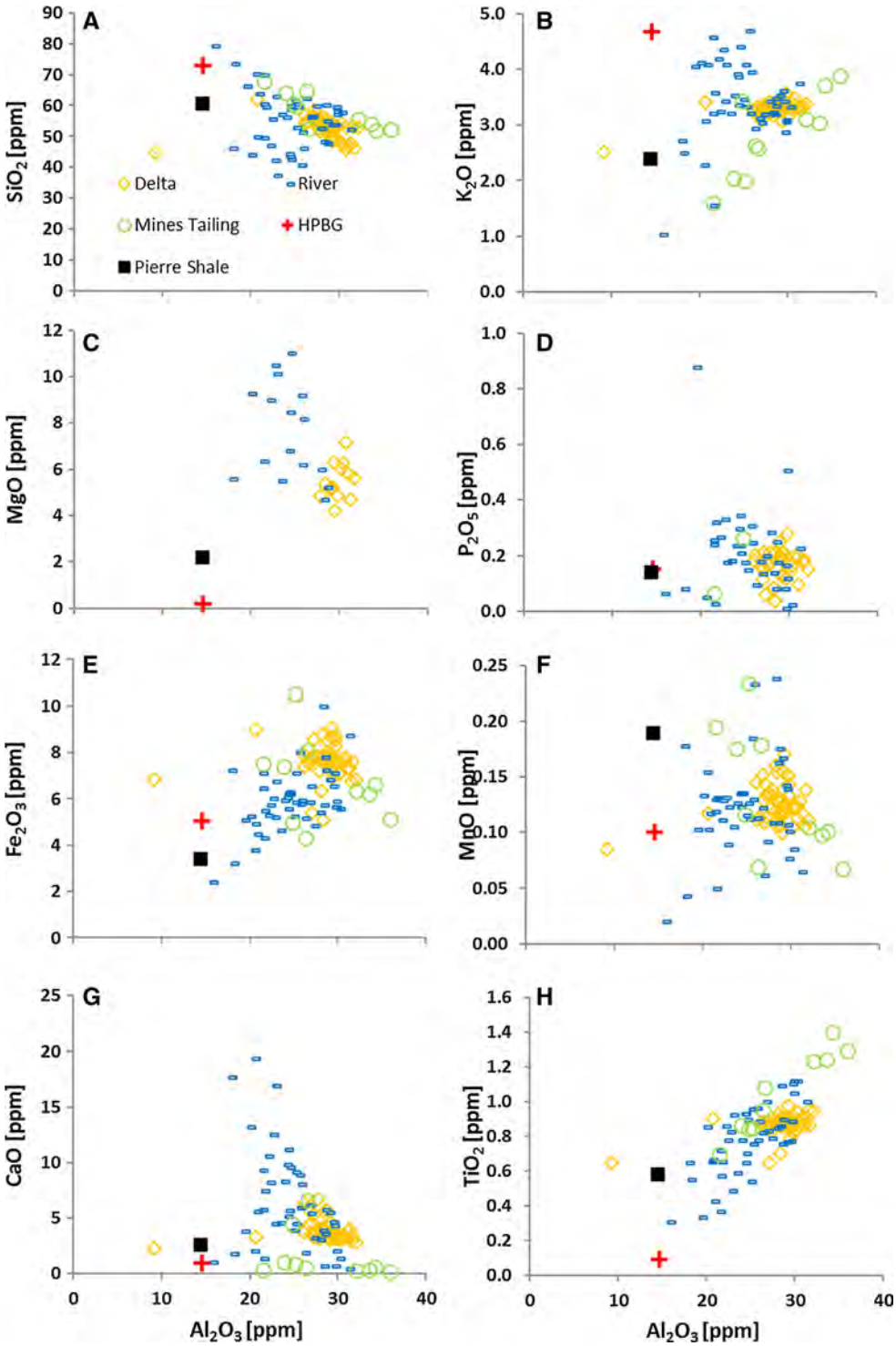

Fig. 3 **a** SiO_2, **b** K_2O, **c** MgO, **d** P_2O_5, **e** Fe_2O_3, **f** MnO, **g** CaO, **h** TiO_2 compared to Al_2O_3 for the study samples. *Red* "+" reference Harney Peak Biotitic Granite (HPBG)

physical weathering, the breakdown of source rocks where sorting of sediment particles during transportation often leads to enrichment of specific minerals (Sensarma et al. 2008; Whitmore et al. 2004). Samples collected between Dead Canyon and Red Canyon exhibited relatively low SiO_2 and Al_2O_3, and relatively high Ca and MgO, consistent with the calcite and Mg common to the in Minnelusa Formation and Minnekahta Limestone common to the southern Black Hills.

The ratio of log Fe_2O_3/K_2O and log SiO_2/Al_2O_3 can discern source mineralogy as well as differentiate between mature and immature unconsolidated sediments (Herron 1988). As shown in Fig. 4 (A) most soil and sediment samples were consistent with the black shales of the Black

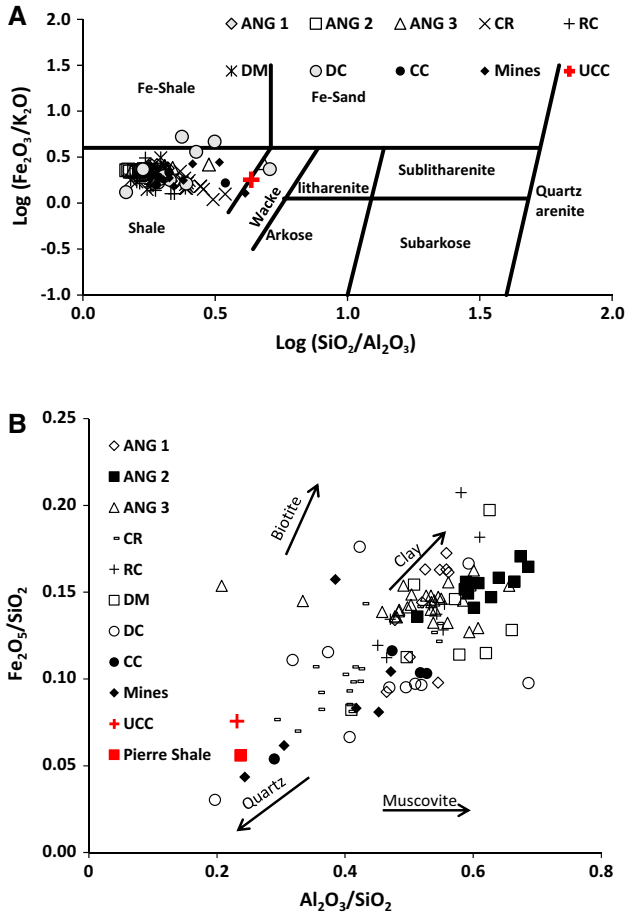

Fig. 4 Chemical maturity and mineral stability (Herron 1988) of the sediments collected from the southern Black Hills region **a** Al_2O_3/SiO_2 versus Fe_2O_3/SiO_2 for soil, Cheyenne River, and Angostura Reservoir delta sediments. Linear trend represent mineralogical sorting. **b** Geochemistry of the sediments collected from the southern Black Hills region compared to UCC and Pierre Shale

Hills region with the exception of Dead Canyon (DC) samples classified as "wacke". Herron's classification also effectively distinguished Fe rich sediments from Dead Canyon. Sediments with lithic particles are commonly referred as immature, consistent with southern Black Hills samples containing the presence of detrital feldspar (Wang et al. 1990). Comparisons with Fe_2O_3/SiO_2 and Al_2O_3/SiO_2 ratios in upper continental crust (UCC) following Galy and France-Lanord (2001) and Pierre Shale from Schultz et al. (1980) (Fig. 4b) indicate Angostura Reservoir delta sediments were enriched in Al and Fe, and depleted in Si compared to Cheyenne River (CR) sediments, UCC and Pierre Shale (PS). This is consistent with the sorting of minerals during transport where base flow sediments become enriched in quartz minerals while suspended sediments become enriched in phyllosilicates. Therefore, it is concluded that the bottom sediments collected from Angostura Reservoir delta generally consist of suspended load from the Cheyenne River and sediment samples collected from Cheyenne River and its drainages were base flow sediments.

Inter-element relations

Pearson correlation results for data for composited Angostura Reservoir delta sediments, Cheyenne River sediments, and abandoned U mine locations and drainages are presented in Table 1. Manganese and Fe are considered emanating from similar geologic media (Singh and Nayak 2009), and exhibit strong inter-correlations (0.597–0.806) for all samples. Similarly, Sr and Ca exhibited strong inter-correlation (0.665–0.801), and appears due to Sr partitioning behavior into calcite-enriched mineral phases (Chen et al. 1999). Angostura Reservoir delta sediments and abandoned U mine locations showed U correlations with V (0.472–0.513), Rb (0.576–0.632), and Mo (0.867–0.948). Uranium was also correlated with TiO_2 in abandoned U mine sites. These correlations may be attributed to the historical mining of carnotite (sandstone type U deposits), corvusite, tyuyamunite, and rauvite deposits within the Edgemont district (Robinson and Gott 1958). For the Cheyenne River sediments, U was correlated with Al (0.639), Mn (0.739.), Fe (0.776), Co (0.798), Zn (0.579), Rb (0.758), and Mo (0.883). A strong correlation of Fe, Ti, Mn, and U with Al_2O_3 found within the Cheyenne River sediments suggests the presence of phyllosilicates, while a Fe and U affinity appears due to the presence of brannerite and samarskite minerals. For the U minesites, a strong negative correlation existed between Sr and SiO_2 and Zr suggesting quartz mineral deficiency, consistent with the mineral sorting of source materials weathering and transport processes.

Trace elements

Base flow sediments generally have high concentrations of trace elements resulting from source rock composition, weathering, and grain size sorting, amongst others (Ayers et al. 2000). Metal pollution assessment of river sediment has utilized heavy metals signatures for provenance determination (Vital and Stattegger 2000; Vital et al. 1999). High field strength elements (HFSE) Zr, Hf, Ti, Pb, and U and transition elements Cr, Mn, Fe, Ni, Cu, and Zn are considered relatively immobile and least soluble trace elements in fairly neutral waters, and if transported as suspended particles, may effectively provide a geochemical signature of the geologic origin.

Average values of soil and sediments collected from the southern Black Hills region were plotted on a Pierre Shale-normalized spider diagram (Fig. 5). These results show similarities for all elements with the exception of

Table 1 Pearson correlation coefficient of chemical data for (A) Angostura Reservoir delta bottom sediments, (B) Cheyenne River bed sediment, and (C) abandoned U mines spoils and drainages sediments

A

	Al_2O_3	SiO_2	P_2O5	K_2O	CaO	TiO_2	MnO	Fe_2O_3	V	Co	Cu	Zn	As	Rb	Sr	Zr	Mo	U
MgO	0.338	-0.579	-0.098	-0.192	-0.218	-0.176	-0.065	-0.038	-0.489	0.068	-0.320	-0.148	-0.148	-0.054	-0.078	-0.071	0.080	0.235
Al_2O_3		-0.106	0.065	0.704	0.026	0.507	0.261	0.015	-0.022	-0.322	-0.184	-0.011	-0.313	0.116	-0.118	-0.003	0.012	0.046
SiO_2			-0.092	0.280	0.213	0.179	0.105	0.157	0.077	-0.218	0.146	-0.019	-0.141	-0.152	0.111	0.124	0.052	0.067
P_2O5				0.093	0.123	-0.006	-0.366	-0.262	0.304	-0.244	0.267	-0.222	-0.606	-0.061	-0.042	-0.013	0.187	0.171
K_2O					0.027	0.723	0.337	0.503	0.133	-0.250	0.116	0.072	-0.220	0.362	0.061	-0.060	0.231	0.286
CaO						0.077	-0.129	-0.084	0.090	0.040	0.223	-0.109	-0.319	-0.253	0.801	0.043	0.004	-0.046
TiO_2							0.099	0.398	0.073	-0.133	0.380	0.188	-0.016	0.595	0.232	-0.009	0.142	0.276
MnO								0.597	-0.060	-0.224	-0.533	0.171	0.258	0.076	-0.050	-0.078	-0.043	-0.049
Fe_2O_3									0.191	0.042	0.065	0.381	0.210	0.593	0.297	-0.372	0.264	0.328
V										-0.072	0.119	0.061	-0.130	0.238	0.207	0.096	0.591	0.513
Co											0.207	0.088	0.288	0.119	0.201	0.108	0.216	0.104
Cu												-0.029	-0.229	0.366	0.405	-0.195	0.098	0.156
Zn													0.227	0.444	0.067	-0.280	-0.030	0.025
As														0.184	-0.054	0.212	0.039	0.049
Rb															0.233	-0.423	0.433	0.576
Sr																-0.112	0.248	0.270
Zr																	0.100	0.017
Mo																		0.948

B

	Al_2O_3	SiO_2	P_2O5	K_2O	CaO	TiO_2	MnO	Fe_2O_3	V	Co	Cu	Zn	As	Rb	Sr	Zr	Mo	U
MgO	-0.863	-0.097	0.989	-0.737	0.888	-0.333	-0.397	0.235	0.000	-1.000	0.809	0.726	--	0.763	0.888	0.925	-1.000	-1.000
Al_2O_3		-0.458	-0.595	-0.255	-0.400	0.711	0.734	0.680	0.008	0.575	-0.055	0.177	-0.159	0.179	-0.208	-0.155	0.380	0.639
SiO_2			0.513	0.556	-0.472	-0.778	-0.588	-0.589	-0.336	-0.293	-0.351	-0.487	0.128	-0.461	-0.588	-0.205	-0.060	-0.346
P_2O5				0.459	-0.099	-0.581	-0.272	-0.288	-0.152	-0.021	-0.096	-0.147	0.583	-0.132	-0.032	0.013	0.036	0.012
K_2O					-0.334	-0.660	-0.092	-0.067	0.034	0.124	-0.159	-0.271	0.016	-0.057	-0.325	-0.215	0.031	-0.040
CaO						0.117	-0.188	-0.199	0.034	-0.337	0.166	0.136	0.046	0.068	0.665	0.246	-0.375	-0.335
TiO_2							0.671	0.619	0.139	0.419	0.317	0.524	0.097	0.443	0.332	0.303	0.130	0.486
MnO								0.806	0.271	0.647	0.299	0.452	0.090	0.495	0.131	0.105	0.446	0.739
Fe_2O_3									0.034	0.778	0.346	0.474	-0.011	0.599	0.220	0.109	0.538	0.776
V										0.028	0.161	0.006	0.146	0.093	0.029	0.014	0.359	0.237
Co											0.701	0.532	-0.220	0.781	-0.025	0.155	0.589	0.798
Cu												0.907	0.852	0.910	0.796	0.884	-0.076	0.582
Zn													0.823	0.934	0.784	0.828	-0.083	0.579
As														0.709	0.615	0.797	-0.523	-0.081
Rb															0.751	0.792	0.113	0.758
Sr																0.770	-0.322	0.027
Zr																	-0.216	0.377
Mo																		0.883

C

	Al_2O_3	SiO_2	P_2O5	K_2O	CaO	TiO_2	MnO	Fe_2O_3	V	Co	Cu	Zn	As	Rb	Sr	Zr	Mo	U
MgO	-0.270	-0.729	0.744	0.866	0.430	0.467	-0.363	-0.379	-0.275	-0.542	-0.512	-0.378	-0.555	0.246	0.421	0.037	0.123	0.263
Al_2O_3		-0.188	0.185	0.294	-0.466	0.889	-0.109	0.281	0.387	0.186	0.258	0.561	-0.138	0.727	-0.188	0.082	0.264	0.427
SiO_2			-0.661	-0.852	-0.732	-0.400	-0.401	-0.463	0.018	-0.163	-0.439	-0.560	0.337	-0.655	-0.754	0.387	-0.073	-0.287
P_2O5				0.641	0.612	0.310	0.207	0.262	-0.212	0.051	0.176	0.437	-0.360	0.551	0.562	-0.364	0.207	0.465
K_2O					0.545	0.468	0.121	0.178	-0.042	-0.170	0.248	0.584	-0.371	0.773	0.621	-0.273	0.037	0.312
CaO						-0.186	0.316	0.132	-0.274	-0.064	0.233	0.073	-0.178	0.111	0.771	-0.440	-0.112	-0.027
TiO_2							0.009	0.318	0.402	0.216	0.261	0.503	-0.298	0.756	-0.027	0.121	0.337	0.549
MnO								0.682	0.003	0.604	0.396	0.231	-0.358	-0.030	0.144	0.080	0.030	-0.013
Fe_2O_3									-0.059	0.818	0.586	0.481	-0.333	0.323	0.251	-0.124	0.190	0.225
V										-0.040	0.002	-0.186	0.115	0.195	-0.458	0.162	0.466	0.472
Co											0.486	0.216	-0.189	0.031	0.027	0.129	0.280	0.179
Cu												0.534	-0.227	0.385	0.307	-0.256	0.003	0.090
Zn													-0.214	0.706	0.365	-0.334	-0.105	0.106
As														-0.280	-0.112	-0.065	-0.103	-0.234
Rb															0.336	-0.312	0.288	0.632
Sr																-0.512	-0.163	-0.008
Zr																	0.064	-0.149
Mo																		0.867

Values shown in gray highlight indicate significant correlation at the 0.05 level

Angostura delta sediments (ANG 2) which had a relatively higher abundance of Hf. All samples were enriched in HFSE and strongly depleted in Ni and Sr, while Cr and Zn were depleted within most samples. These patterns are consistent with the detrital component of sediments transported from source areas, possibly due to anthropogenic processes such as mining. Transport mechanisms of reservoir sediments can alter the composition of immobile

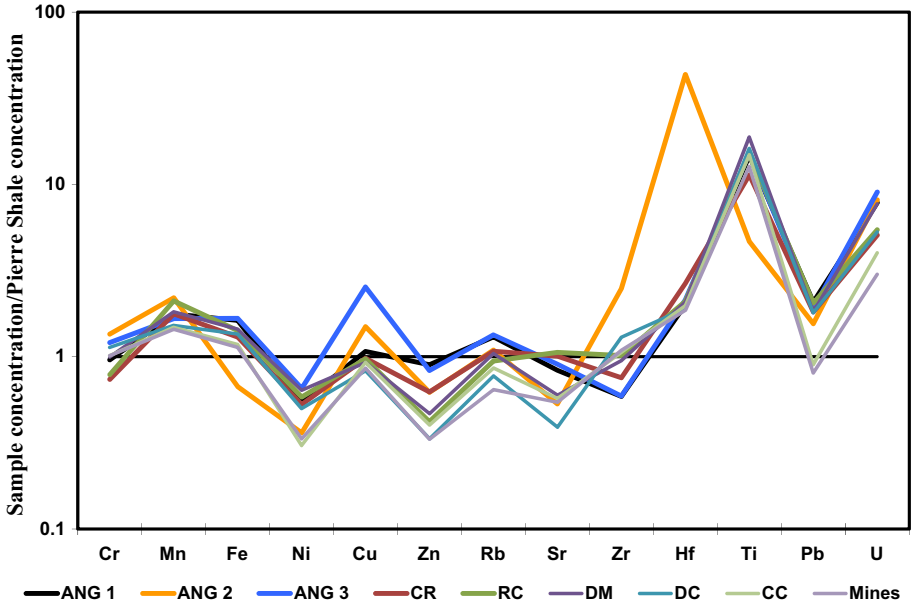

Fig. 5 Pierre Shale-normalized spider diagram of reservoirs in the southern Black Hills region. Sample locations arranged from closest to the Angostura Reservoir (ANG) to the farthest away (mines)

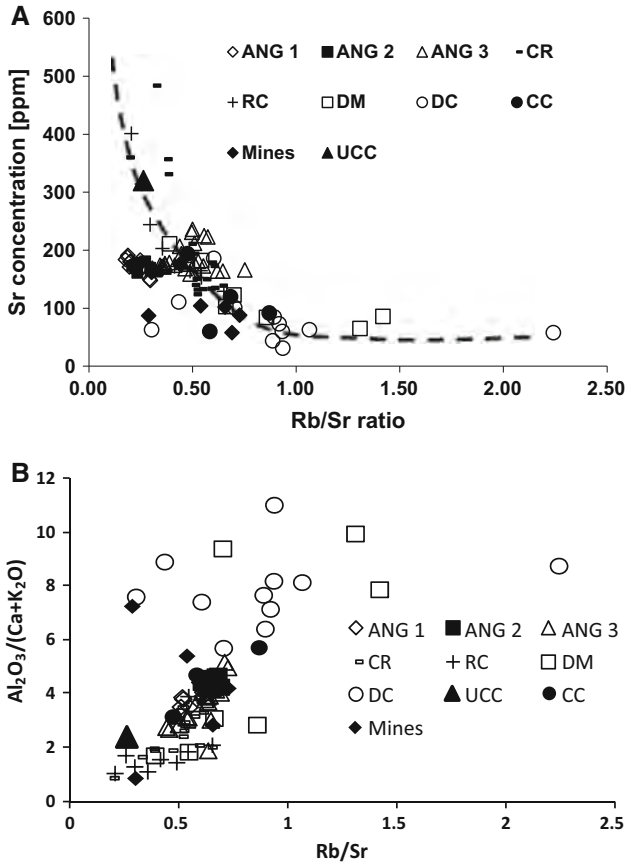

Fig. 6 **a** Rb/Sr ratio of the sediments of southern Black Hills region. *Dashed line* present Sr enrichment zone and **b** comparison between Rb/Sr ratio and $Al_2O_3/(CaO + K_2O)$ the sediments of southern Black Hills region

trace elements; however, inter-elemental ratios are largely controlled by the source material signatures (Borges et al. 2008).

The Rb/Sr ratios of the sediments have been effectively used to describe weathering intensities from a catchment (Walther 2009; Chen et al. 1999; Jin et al. 2006; Rasbury et al. 2012; Xu et al. 2010), and provide a mechanism to understand metal transport mechanisms. Large ion lithosphere elements (LILE) such as Rb tend to have differing relations and mineral structures compared to Sr, typically considered fluid-mobile and subject to weathering (Walther 2009). For example, Rb substitutes for K in the K-feldspar, resulting in increasing the Rb/Sr ratio of the residue (Walther 2009). Similarly, when plagioclase crystallizes, Ca becomes incorporated into Sr, resulting in decreased Rb/Sr ratio. Rubidium generally coexists with K-rich minerals and Sr incorporated in Ca and Na-bearing minerals (Chen et al. 1999; Xu et al. 2010). Calcium and Na minerals are more reactive to the weathering then K-rich minerals, where weathering readily removes Ca and Na bearing minerals from paleosols leading to residues enriched in Rb but depleted in Sr. Low Sr concentration commonly result in high Rb/Sr ratios, suggesting weak chemical weathering, while high Sr (low Rb/Sr) may be indicative of strong chemical weathering. Shale rock has relatively higher Rb/Sr ratio compared to weathered rock (Rasbury et al. 2012).

The Sr concentration in sediments was generally depleted compared to UCC, suggesting physical weathering was a dominant factor within the study area (Fig. 6a).

Table 2 Average concentration (ppm) (A) and standard deviation (B) of heavy metals for the study sites

	V		Cu		Zn		As		Zr		Mo		U	
	A	B	A	B	A	B	A	B	A	B	A	B	A	B
ANG 1	**112.1**	92.57	35.2	5.96	**81.1**	19.74	10	5.93	138	51.48	67.6	30.24	**46.5**	20.68
ANG 2	**130.9**	71.43	36.5	5.43	**95.2**	31.22	8.1	4.64	113.5	8.47	64.6	21.48	**45.5**	13.08
ANG 3	**129.2**	76.89	**86.3**	23.94	**88.1**	5.38	7.2	4.37	114	8.81	70.9	22.23	**52.4**	14.49
CR	67.1	41.77	33.3	17.27	**66.2**	41.25	9.7	8.65	145.7	71.11	47.9	25.19	29.5	16.23
RC	41.7	44.23	33	6.56	44.6	13.92	7.1	4.98	**196.1**	39.87	55.1	22.37	31.7	14.35
DM	**108**	91.06	31.4	3.69	49.6	17.00	5.2	3.60	**183**	24.27	71.1	29.05	**44.7**	29.23
DC	81.4	48.46	28.2	5.84	35.4	12.04	6.3	4.79	**250.6**	69.08	59.4	18.75	30.7	20.81
CC	40.8	43.58	31.5	3.11	42.5	12.34	11.3	8.39	**204.8**	67.01	50.8	3.77	23.3	12.76
Mines	**108**	77.36	29.1	5.34	35.1	14.09	13.3	12.99	**210.4**	54.61	49.4	3.99	17.4	8.50

Values shown in bold highlight present elevated concentration

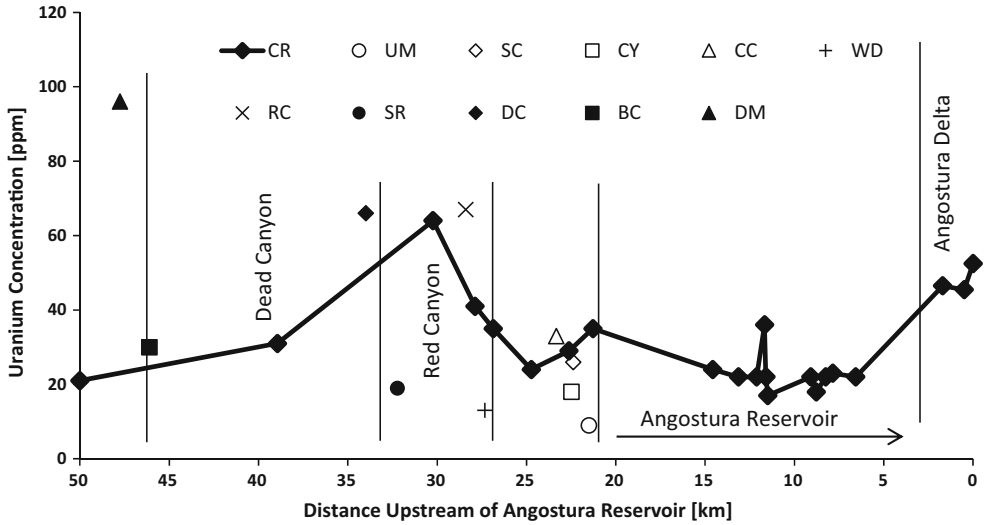

Fig. 7 Uranium concentration as a function of distance upsteam of Angostura Reservoir along the Cheyenne River

Few Cheyenne River sediments exhibited high Sr content suggesting a strong chemical weathering signature from sedimentary sorting occurred. Shallow depth sediments collected from Angostura Reservoir delta (ANG 1) have low Rb/Sr ratio and higher Sr concentration compared to UCC, further suggesting a strong chemical weathering signature for the catchment. Samples collected from Dead Canyon (DC), Dewey Mines (DM), and Chilson Canyon (CC) exhibited high Rb/Sr ratios and low Sr concentrations compared to UCC, suggest a strong physical weathering signature. The average Rb/Sr ratios for the Angostura Reservoir delta bottom sediments was 0.37, which was higher than the average Rb/Sr ratio of UCC (0.26); however, it was lower than average Rb/Sr ratio for the Cheyenne River catchment sediments (0.49). These findings suggest the Cheyenne River sediments were leached more during transportation processes (Xu et al. 2010), and having undergone a weak chemical weathering process in arid and cold climate (Zhangdong et al. 2001).

The ratio of $Al_2O_3/(CaO + K_2O)$ is an alternative way to describe the weathering intensity in a watershed. This ratio is calculated by normalizing immobile Al_2O_3 with mobile elements CaO and K_2O. Comparison between Rb/Sr and $Al_2O_3/(CaO + K_2O)$ show a linear trend which shows a correlation between these two ratios (Fig. 6b). Samples collected from the Mines, Dead Canyon, Dewey Mines, and Chilson Canyon have higher $Al_2O_3/(CaO + K_2O)$ and a Rb/Sr ratio depicting weak chemical weathering in the mining areas.

Assessment of metal contamination

Average composition and standard deviation of heavy metals concentrations for all soil and sediment samples

Table 3 Enrichment factors (EF) of heavy metals in the southern Black Hills region

Sample	Mn	Fe	Cu	Zn	Rb	Sr	Zr	U
DM	0.70	0.30	0.60	0.40	0.56	0.20	0.51	8.88
DC	0.62	0.29	0.58	0.30	0.44	0.14	0.74	6.49
RC	0.99	0.32	0.77	0.43	0.61	0.44	0.66	7.62
CC	0.63	0.25	0.67	0.37	0.51	0.22	0.63	5.09
Mines	0.69	0.27	0.69	0.35	0.43	0.23	0.73	4.30
CR	0.82	0.35	0.76	0.63	0.69	0.41	0.48	6.98
ANG 3	0.67	0.33	1.72	0.73	0.74	0.32	0.33	10.83
ANG 2	0.65	0.31	0.67	0.73	0.67	0.27	0.30	8.65
ANG 1	0.77	0.32	0.68	0.65	0.65	0.29	0.39	9.31

collected are presented in Table 2. Delta sediments of Angostura Reservoir were markedly enriched in V, Zn, and U. Uranium was also elevated from the mine spoil and drainages at near U Mines sampled near Dewey (Fig. 2). Uranium concentrations in sediment samples collected from the Cheyenne River catchment were generally higher (22 ppm average) in the upstream sediments compared to those nearest Angostura Reservoir (14 ppm average) (Fig. 7). Molybdenum was enriched (47.9–71.1 ppm) for all samples compared to the HPBG (3.2 ppm), and correlate to known carbonaceous and pyritic shale concentration (100 ppm) (Kuroda and Sandell 1954). Molybdenum concentrations were variable, likely attributed to adsorption by Fe in deeper sediments where concentration of dissolved sulfide is higher, and thus is difficult to estimate Mo within sedimentary rocks (Chappaz et al. 2008). With the exception of Zn, all sediment samples collected from Cheyenne River were comparable to UCC (67 ppm) range, however, were enriched compared to HPBG (27.5 ppm). Zirconium was elevated from abandoned U mine regions, Dead Canyon, and Chilson Canyon. Placer deposits of U bearing minerals are known to have elevated Th and Zr (Butler 1952), consistent with the presence of Carnotite minerals common to the Inyan Kara formations of the southern Black Hills. Generally, elevated heavy metal concentration existed in both the upper and lower reaches of the Cheyenne River catchment, with higher concentrations within the upper reaches indicative of rapid sedimentation processes. Episodic flooding events appear to transport contaminated sediments from the minesites and surrounding areas effectively, with very little accumulation or contaminant signature existing along the intermediate watercourse.

Enrichment factors and pollution load indices

The major source of heavy metal concentration in the aquatic system is typically river sediments derived from the

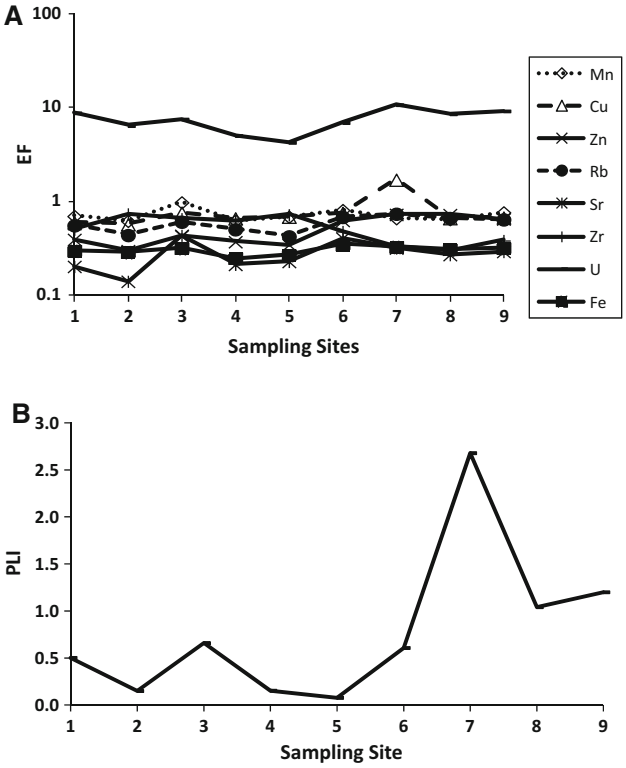

Fig. 8 **a** Enrichment factor of sediment elements, and **b** pollution load index for the study sites. Sample sites: *1* DM, *2* DC, *3* RC, *4* CC, *5* mines, *6* CR, *7* ANG 3, *8* ANG 2, *9* ANG 1, where sample number 9 being the closest to the Angostura Reservoir and sample 1 the farthest upstream

Table 4 Contamination factors (CF) and pollution load index (PLI) signifying degree of sediment contamination for the study sites

Sample	Mn	Fe	Cu	Zn	Rb	Sr	Zr	U	PLI
DM	1.31	0.54	1.12	0.74	1.04	0.38	0.95	16.56	0.50
DC	1.09	0.49	1.01	0.53	0.77	0.25	1.30	11.36	0.15
RC	1.52	0.48	1.18	0.67	0.94	0.68	1.02	11.73	0.66
CC	1.06	0.42	1.13	0.63	0.86	0.36	1.06	8.61	0.15
Mines	1.04	0.39	1.04	0.52	0.64	0.35	1.09	6.46	0.08
CR	1.28	0.54	1.19	0.99	1.08	0.64	0.76	10.91	0.61
ANG 3	1.20	0.58	3.08	1.32	1.34	0.58	0.59	19.42	2.68
ANG 2	1.27	0.59	1.30	1.42	1.30	0.53	0.59	16.84	1.04
ANG 1	1.43	0.58	1.26	1.21	1.20	0.55	0.72	17.22	1.20

weathering of rocks and soils within a drainage basin. Other common sources may include anthropogenic factors such as mining activities, waste water discharge, agriculture activities, and urban/suburban stormwater runoff. Suspended sediments are the predominant source of heavy metal loadings within aquatic system (Chakravarty and Patgiri 2009). The geochemistry of river and delta sediments assists with quantifying and understanding pollution trends in water systems. One valuable method of

impairment assessment is the determination of enrichment factors (EF). The EF were determined for Mn, Fe, Cu, Zn, Rb, Sr, Zr, and U in this study (Table 3; Fig. 8). With the exception of Cu in ANG 3 (1.72) sediments and U in all soil and sediment samples, all samples indicated EF depletion (<1). With the exception of Mines samples, most downstream sediments were enriched in U further signifying pollution migration from the upper catchment reaches.

Pollution load index (PLI) is another accepted sediment environmental impacts assessment methodology for quantifying anthropogenic activities (Tomlinson et al. 1980). All sediment and soil samples exhibited low PLI with the exception of sediments from the Angostura Reservoir (ANG 3) which were relatively high (2.68) (Table 4). There was generally an increase in PLI as one travels downstream of the Cheyenne River (Fig. 8) and appears to coincide sediment (and pollution) transport from the upper catchment mine sites. Contamination factors for U was elevated for all sites, including the Dewey U Mines (16.56), Cheyenne River (10.91), and Angostura delta (16.84–19.42). These findings further support that Angostura Reservoir U loading appears attributed to suspended particle transport from the upper Cheyenne River catchment, including areas impacted by historical U mining activities in the region.

Conclusion

Geochemical analysis of bottom sediments, sediment, and soil samples from Angostura Reservoir delta, Cheyenne River, and abandoned U mine regions indicate that U concentration found within these locations were elevated compared to regional Pierre Shale concentrations. The highest U concentrations were found in the abandoned U mine areas, and within the Angostura Reservoir delta samples. The highest PLIs determined for the study were those associated with Angostura Reservoir delta sediments (ANG 3), suggesting that the Cheyenne River is an effective transporter of contaminants from the upper catchment reaches. There was little evidence of contaminant accumulation within Cheyenne River reaches, and instead the mobile contaminants appear effectively conveyed the Angostura Reservoir. Heavy metals appear to remain as suspended load within the Cheyenne River, as evident of increasing EF and PLI values within its reach. Anthropogenic activities such as historic U mining appear to be a significant contributor to contaminant loading within this historical mining area catchment.

Acknowledgments This research was supported by the US Environmental Protection Agency—Region 8 and the US Department of Agriculture/Forest Service—Northern Region (Robert Wintergerst) is gratefully acknowledged. We would also like to thank SDSM&T students Bryce Pfeifle, Gregory Delzer, and Ashwin Karunaratna for their assistance.

References

Ayers MA Kennen JG, Stackelberg PE (2000) Water quality in the long island—New Jersey coastal drainages New Jersey and New York, 1996–98. Geological Survey circular, vol 1201, p 40

Borges JB, Huh Y, Moon S, Noh H (2008) Provenance and weathering control on river bed sediments of the eastern Tibetan Plateau and the Russian Far East. Chem Geol 254(1–2):20

Braddock WA (1955) Map showing distribution and occurrences of uranium deposits in part of the Edgemont mining district, Fall River County, South Dakota. Miscellaneous Field Studies Map, vol 39. Geological Survey, Reston

Butler AP Jr (1952) The Geological Survey's work on the geology of uranium and thorium deposits. USGS Numbered Series, vol 207. US Geological Survey, p 30

Chakravarty M, Patgiri AD (2009) Metal pollution assessment in sediments of the Dikrong River, N.E. India. J Hum Ecol 27(1):5

Chappaz A, Gobeil C, Tessier A (2008) Geochemical and anthropogenic enrichments of Mo in sediments from perennially oxic and seasonally anoxic lakes in Eastern Canada. Geochim Cosmochim Acta 72(1):170–184

Chen J, An Z, Head J (1999) Variation of Rb/Sr ratios in the loess-paleosol sequences of central China during the last 130,000 years and their implications for monsoon paleoclimatology. Quatern Res 51(3):215–219

Das B, Haake B-G (2003) Geochemistry of Rewalsar Lake sediment, Lesser Himalaya, India: implications for source-area weathering, provenance and tectonic setting. Geosci J 7(4):299–312

Das BK, Al-Mikhlafi AS, Kaur P (2006) Geochemistry of Mansar Lake sediments, Jammu, India: implication for source-area weathering, provenance, and tectonic setting. J Asian Earth Sci 26(6):649–668

Davis AD, Webb CJ (1999) Impacts of abandoned mines on water quality in the Black Hills: a watershed approach. Paper presented at the Black Hills hydrology conference, Rapid City

DeWitt E, Buscher DP (1988). Map of mines, prospects, and classification of mineral deposits in the Edgemont Northwest, 7 1/2 minute quadrangle, Black Hills, South Dakota. Open filed report 87-261-1. US Geological Survey, Reston

Duke EF, Papike JJ, Laul JC (1992) Geochemistry of a boron-rich peraluminous granite pluton: the calamity peak layered granite-pegmatite complex, Black Hills, South Dakota. Can Mineral 30:22

Finnell TL, Parrish IS (1958) Uranium deposits and principal ore-bearing formations of the central cordilleran foreland region. Mineral inversion field studies map, vol 120. US Geological Survey, Reston

Galy A, France-Lanord C (2001) Higher erosion rates in the Himalaya: geochemical constraints on riverine fluxes. Geology 29(1):23–26

Hall RL (1982) Radiological and environmental assessment of the abandoned uranium mines in the Edgemont mining district South Dakota. MS thesis, South Dakota School of Mines and Technology, Rapid City

Heiri O, Lotter AF, Lemcke G (2001) Loss on ignition as a method for estimating organic and carbonate content in sediments: reproducibility and comparability of results. J Paleolimnol 25:101–110

Herron MM (1988) Geochemical classification of terrigenous sands and shales from core or log data. J Sediment Petrol 58(5):820–829

IAEA (1985) Geological environments of sandstone type uranium deposits, vol IAEA-TECDOC-328. International Atomic Energy Agency

Jin ZD, Cao JJ, Wu J, Wang S (2006) A Rb/Sr record of catchment weathering response to Holocene climate change in Inner Mongoli. Earth Surf Proc Land 31:285–291

Kuroda PK, Sandell EB (1954) Geochemistry of molybdenum. Geochim Cosmochim Acta 6(1):35–63

Mmolawa KB, Likuku AS, Gaboutloeloe GK (2011) Assessment of heavy metal pollution in soils along major roadside areas in Botswana. Afr J Environ Sci Technol 5(5):10

Osterwald FW, Dean BG (1961) Relation of uranium deposits to tectonic pattern of the central Cordilleran foreland. USGS Numbered Series, vol 1087-I. US Geological Survey, Reston, pp 337–390

Rahn PH, Hall RL (1982) A reconnaissance inventory of environmental impacts of uranium mining in the Edgemont mining district, Fall River County, South Dakota. Rocky Mountain Forest and Range Experiment Station, US Forest Service, p 54

Rahn PH, Davis AD, Webb CJ, Nichols AD (1996) Water quality impacts from mining in the Black Hills, South Dakota, USA. Environ Geol 27(1):38–53

Rasbury ET, Hemming SR, Rigge NR (2012) Mineralogical and geochemical approaches to provenance, vol 487. GSA Special Papers

Rich FJ (1981) Geology of the Black Hills, South Dakota and Wyoming. American Geological Institute, p 31

Robinson CS, Gott GB (1958) Uranium deposits of the Black Hills South Dakota and Wyoming. Trace elements investigations report, vol 723. US Geological Survey, Reston, p 13

Sales JK (1968) Crustal mechanics of cordilleran foreland deformation: a regional and scale-model approach. AAPG Bull 52(10):28

Schultz LG, Tourtelot HA, Gill JR, Boerngen JG (1980) Composition and properties of the Pierre Shale and equivalent rocks. Northern Great Plains Region, vol 1064-B. US Geological Survey, Reston, p 123

Sensarma S, Rajamani V, Tripathi JK (2008) Petrography and geochemical characteristics of the sediments of the small River Hemavati, Southern India: implications for provenance and weathering processes. Sed Geol 205(3–4):111–125

Sinex SA, Helz GR (1981) Regional geochemistry of trace elements in Chesapeake Bay sediments. Environ Geol 3(6):315–323

Singh KT, Nayak GN (2009) Sedimentary and geochemical signatures of depositional environment of sediments in mudflats from a microtidal kalinadi estuary, central west coast of India. J Coastal Res 25(3):11

Tomlinson DL, Wilson JG, Harris CR, Jeffrey DW (1980) Problems in the assessment of heavy-metal levels in estuaries and the formation of a pollution index. Helgoländer Meeresuntersuchungen 33(1–4):566–575

Vital H, Stattegger K (2000) Major and trace elements of stream sediments from the lowermost Amazon River. Chem Geol 168(1–2):151–168

Vital H, Stattegger K, Garbe-Schoenberg CD (1999) Composition and trace-element geochemistry of detrital clay and heavy-mineral suites of the lowermost Amazon River; a provenance study. J Sediment Res 69(3):563–575

Walther JV (2009) Essentials of geochemistry, 2nd edn. Jones and Bartlett, Burlington

Wang KY, Windley BF, Sills JD, Yan YH (1990) The Archaean gneiss complex in E. Hebei province, north China: geochemistry and evolution. Precambr Res 48:20

Webb CJ, Davis AD, Paterson CJ (1998) Comprehensive inventory of known abandoned mine lands in the Black Hills of South Dakota. Min Eng 50(7):3

Whitmore GP, Crook KAW, Johnson DP (2004) Grain size control of mineralogy and geochemistry in modern river sediment, New Guinea collision, Papua New Guinea. Sediment Geol 171(1–4):129–157

Windom HL (1988) A guide to the interpretation of metal concentrations in estuarine sediments. Skidaway Institute of Oceanography, Savannah

Xu H, Liu B, Wu F (2010) Spatial and temporal variations of Rb/Sr ratios of the bulk surface sediments in Lake Qinghai. Geochem Trans 11(1):3

Webb CJ, Davis AD, Hodge VF (1995) Rare earth elements at abandoned uranium mines in the southern Black Hills of South Dakota. Society for Mining, Metallurgy, and Exploration, p 4

Zhangdong J, Sumin W, Ji S, Enlou Z, Fuchun L, Junfeng J et al (2001) Weak chemical weathering during the Little Ice Age recorded by lake sediments. Sci China 44(7):7

Zoller WH, Gladney ES, Duce RA (1974) Atmospheric concentrations and sources of trace metals at the South Pole. Science 183(4121):198–200